SUPPLEMENTAL FIGURE LEGENDS

Supplemental Figure 1. microCT imaging illustrates exacerbated phenotype in *Notch1*$^{+/-}$;*Fbn1*$^{C1039G/+}$ mice. (**A-B**) Representative images from microCT anaylsis. (**C-L**) Quantification of aortic diameter showing increased dilation in the ascending aorta (**C-H**) of *Notch1*$^{+/-}$;*Fbn1*$^{C1039G/+}$ mice in comparison to Fbn1$^{C1039G/+}$ mice with both maximal (**C-E**) and orthogonal (**F-H**) measurements. These differences were not observed in the descending aorta (**I-L**). (**M**) Diagram of maximal and orthogonal measurements. WT, wildtype; N, *Notch1*$^{+/-}$; F, *Fbn1*$^{C1039G/+}$; NF, *Notch1*$^{+/-}$;*Fbn1*$^{C1039G/+}$

Supplemental Figure 2. Blood pressure changes are not responsible for exacerbated phenotype.

Blood pressure differences were not observed between *Fbn1*$^{C1039G/+}$ mice and *Notch1*$^{+/-}$;*Fbn1*$^{C1039G/+}$ mice. Blood pressure was significantly lower in *Notch1*$^{+/-}$ mice than wildtype mice. Student t-test was used to determine significance. *p<0.05.

Supplemental Figure 3. Summary of *Notch1* specific deletions in mature smooth muscle cells, smooth muscle precursor cells, and cardiac neural crest. (**A**) Quantification of echocardiographic analysis detailing aortic diameter at 4 locations in the thoracic aorta. No differences were observed between groups. STJ, sinotubular junction; AscAo, ascending aorta. (*Notch1*$^{+/fl}$;*Fbn1*$^{C1039G/+}$, n=9; *Notch1*$^{+/fl}$;*Myh11-Cre*$^{+/-}$;*Fbn1*$^{C1039G/+}$, n=17). (**B**) Quantification of echocardiographic analysis detailing aortic diameter at 4 locations in the thoracic aorta. No differences were observed between

groups. (*Notch1*$^{+/fl}$;*Fbn1*$^{C1039G/+}$, n=5; *Notch1*$^{+/fl}$;*Wnt1-Cre*$^{+/-}$;*Fbn1*$^{C1039G/+}$, n=10). (**C**) Quantification of echocardiographic analysis shows that *Fbn1*$^{C1039G/+}$ mice with heterozygous deletion of *Notch1* specifically in smooth muscle precursor cells with *Myocd-Cre*$^{+/-}$ mice recapitulates the aortic root dilation observed in the *Notch1*$^{+/-}$;*Fbn1*$^{C1039G/+}$ mice (*Notch1*$^{+/fl}$;*Fbn1*$^{C1039G/+}$, n=5; *Notch1*$^{+/fl}$;*Myocd-Cre*$^{+/-}$;*Fbn1*$^{C1039G/+}$, n=4).

Supplemental Figure 4. Second heart field-specific knock-out of *Notch1* results in cardiac outflow tract defects. Hematoxylin and eosin stained E15.5 hearts from (**A-B**) wildtype and (**C-E**) *Notch1*$^{SHF-KO}$ embryos showing double outlet right ventricle with ventricular septal defect with second heart field-specific knock-out of *Notch1. *, aortic valve; ^, ventricular septal defect; Ao, aorta; PT, pulmonary trunk; RV, right ventricle, LV, left ventricle; RA, right atrium; LA, left atrium.* (**F-G**) Despite outflow tract defects, embryos maintained normal size. (**H-I**) Immunofluorescent staining shows expression of Jag1 and NICD1 in the aortic sac (AS) and aorticopulmonary septum (arrowhead). White dotted line outlines area of low Jag1 expression and higher NICD1 expression, while both proteins are co-expressed surrounding the aortic sac.

Supplemental Figure 5. Second heart field-specific knock-out of *Notch1* results in anomalous aortic development and dilation of the sinotubular junction (STJ) by 1-2 months of age. (**A**) Quantification of echocardiographic analysis detailing aortic diameter at 4 locations in the ascending aorta of Notch1^{SHF-KO} mice at 1-2 months of age. STJ, sinotubular junction; AscAo, ascending aorta. (**B**) Diameter ratio of STJ:sinus

measurements from A. As values approach 1, definition is lost between the sinus and the STJ. (**C-D**) Representative echocardiographic images showing STJ effacement and tortuous aorta. (**E-F**) Gross aortic images showing aortic tortuosity and improper placement of left common carotid artery and left subclavian artery. Student t-test was used to determine significance, which was defined as $p < 0.05$.

Supplemental Figure 6. Lineage tracing of the second heart field reveals a decrease in second heart field-derived smooth muscle cells in *Notch1*$^{+/SHFdel}$ mice. *Notch1*$^{+/SHFdel}$ mice were bred with *ROSA26*$^{mT/mG}$ mice or *R26R* mice in order to perform lineage tracing on second heart field-derived cells. (**A**) Immunofluorescent images of control (*Mef2C-Cre*$^{+/-}$*;ROSA26*$^{mT/mG}$) and second heart field-specific *Notch1* heterozygote (*Notch1*$^{+/fl}$*;Mef2C-Cre*$^{+/-}$*;ROSA26*$^{mT/mG}$) mice showing cells that have been derived from the second heart field via GFP signal. Smooth muscle cells are labeled with Acta2 (n=3/genotype). (**B**) Whole hearts from *Mef2C-Cre*$^{+/-}$*;R26R*$^{+/-}$ and *Notch1*$^{+/fl}$*;Mef2C-Cre*$^{+/-}$*;R26R*$^{+/-}$ mice were assayed for beta-galactosidase activity. A decrease in SHF-derived cells in the aorta and pulmonary trunk is observed with *Notch1* heterozygosity. Scale bars, 200μm.

Supplemental Figure 7. Notch1 expression detected in human AscAA tissue. In comparison to **(A)** normal ascending aorta (control, n=5), visualization of activated Notch1 by immunohistochemistry shows increased expression in **(B-E)** diseased ascending aortic aneurysm samples as the diameter of the aorta increases (n=8). MFS, Marfan syndrome; BAV, bicuspid aortic valve. Scale bar, 200μm.

Supplemental Video 1. 3D reconstruction of wildtype mouse.

Supplemental Video 2. 3D reconstruction of *Notch1*$^{+/-}$;*Fbn1*$^{C1039G/+}$ mouse.

Supplemental Video 3. 3D reconstruction of wildtype great vessels.

Supplemental Video 4. 3D reconstruction of *Notch1*$^{+/-}$;*Fbn1*$^{C1039G/+}$ great vessels.

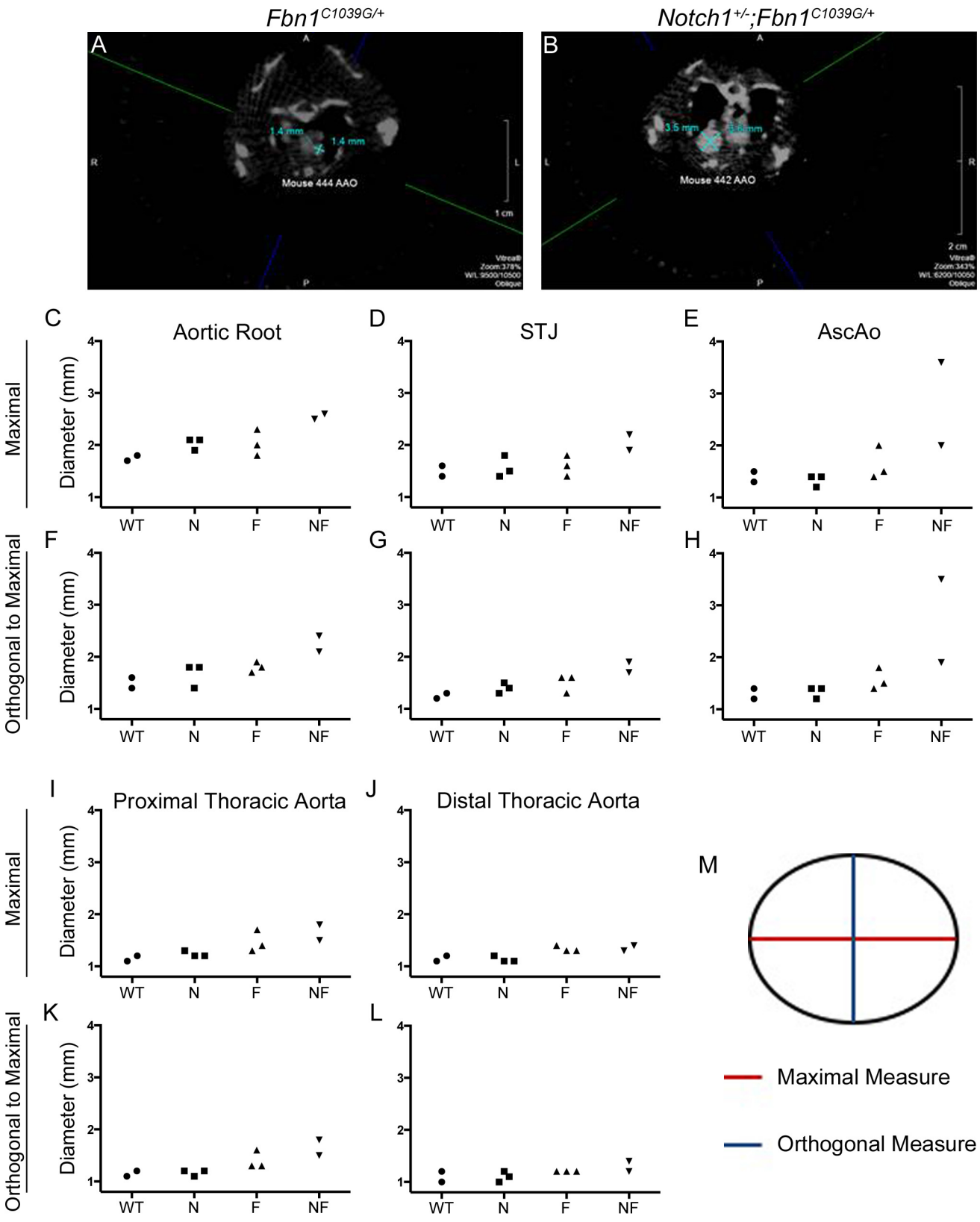

Supplemental Figure 1

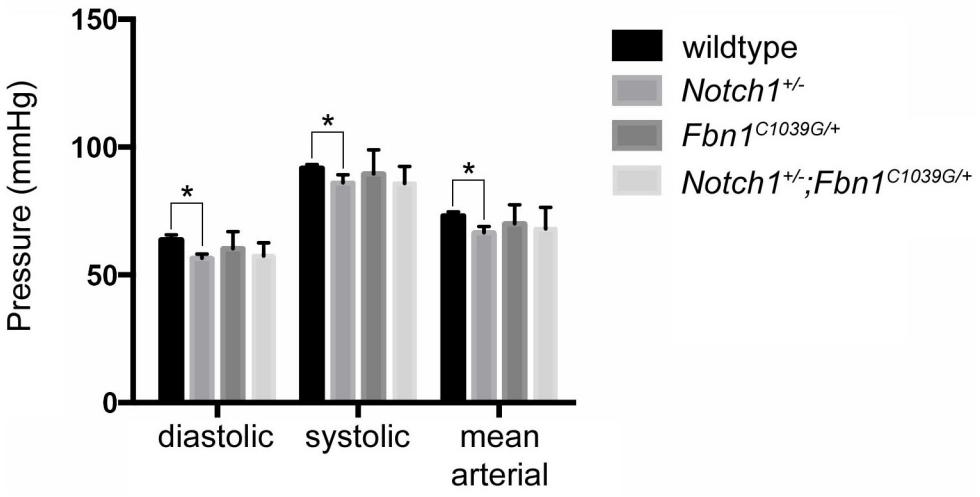

Supplemental Figure 2

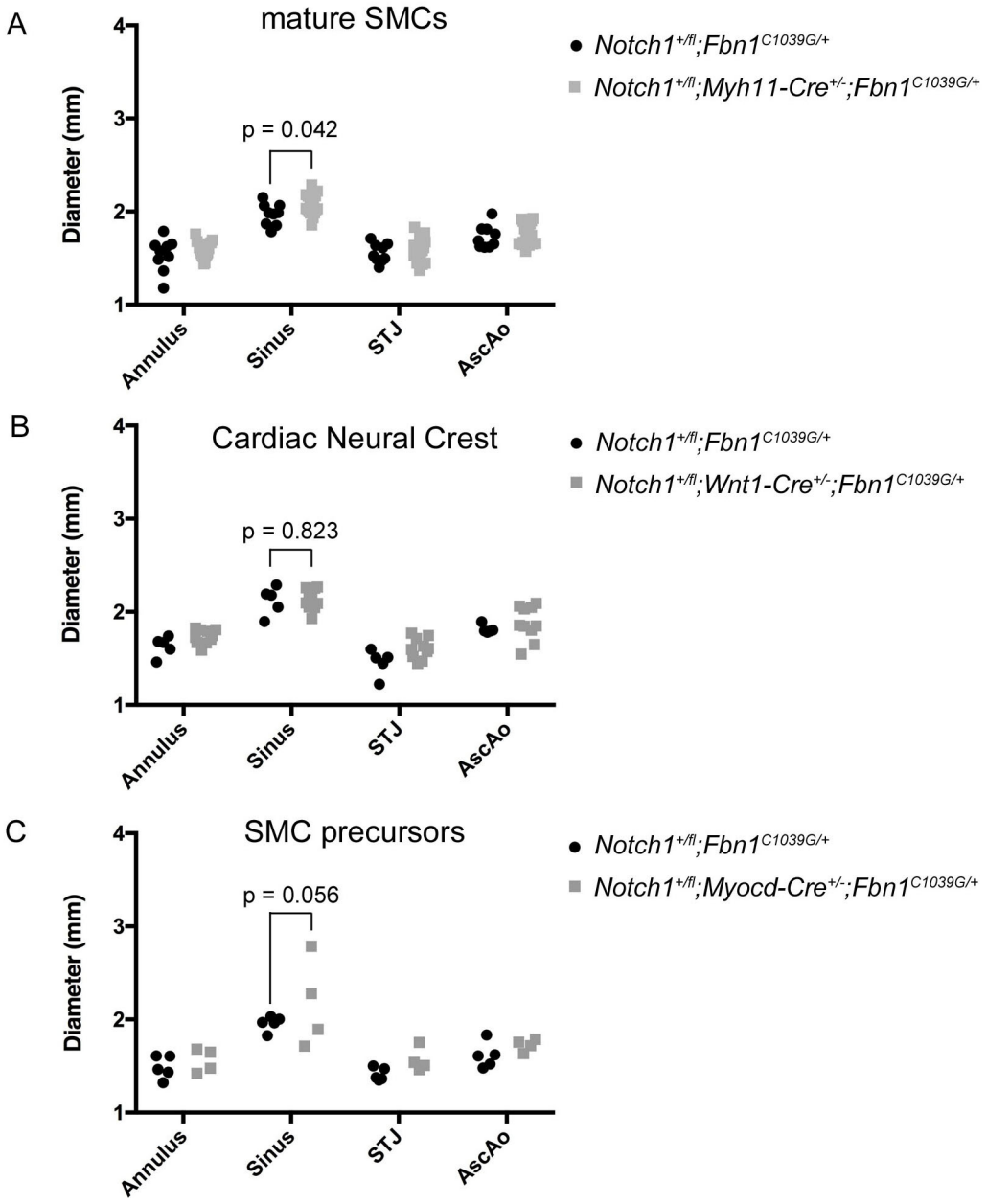

Supplemental Figure 3

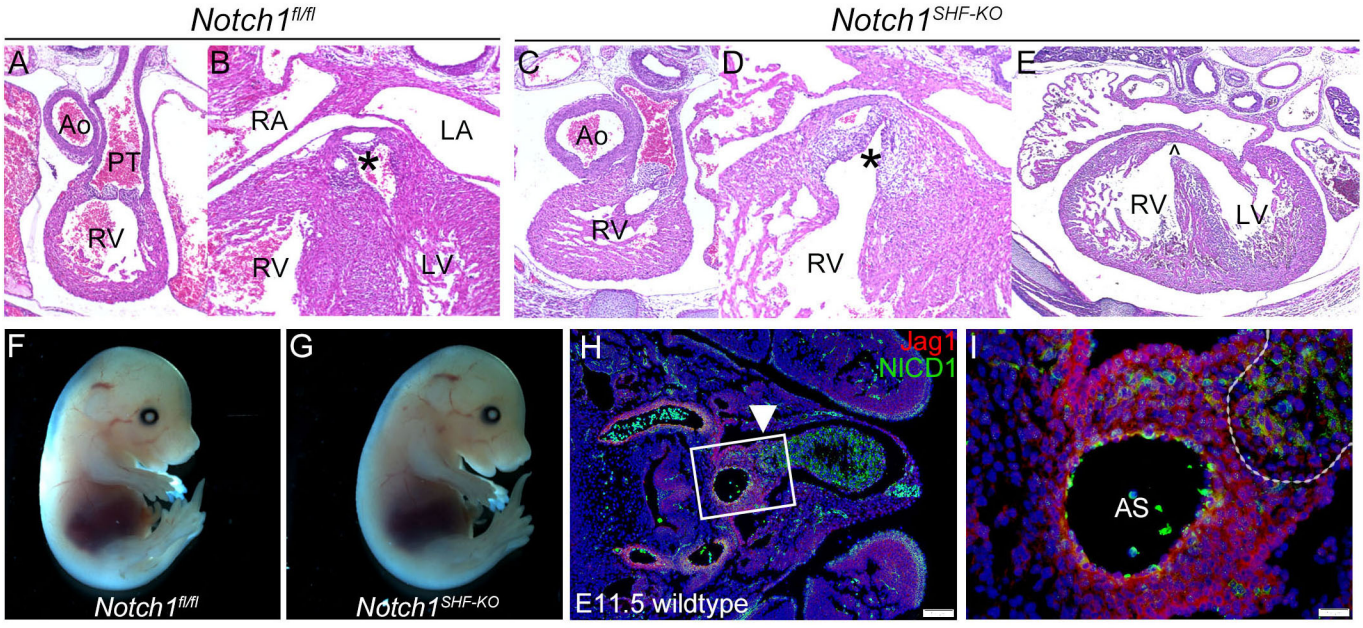

Supplemental Figure 4

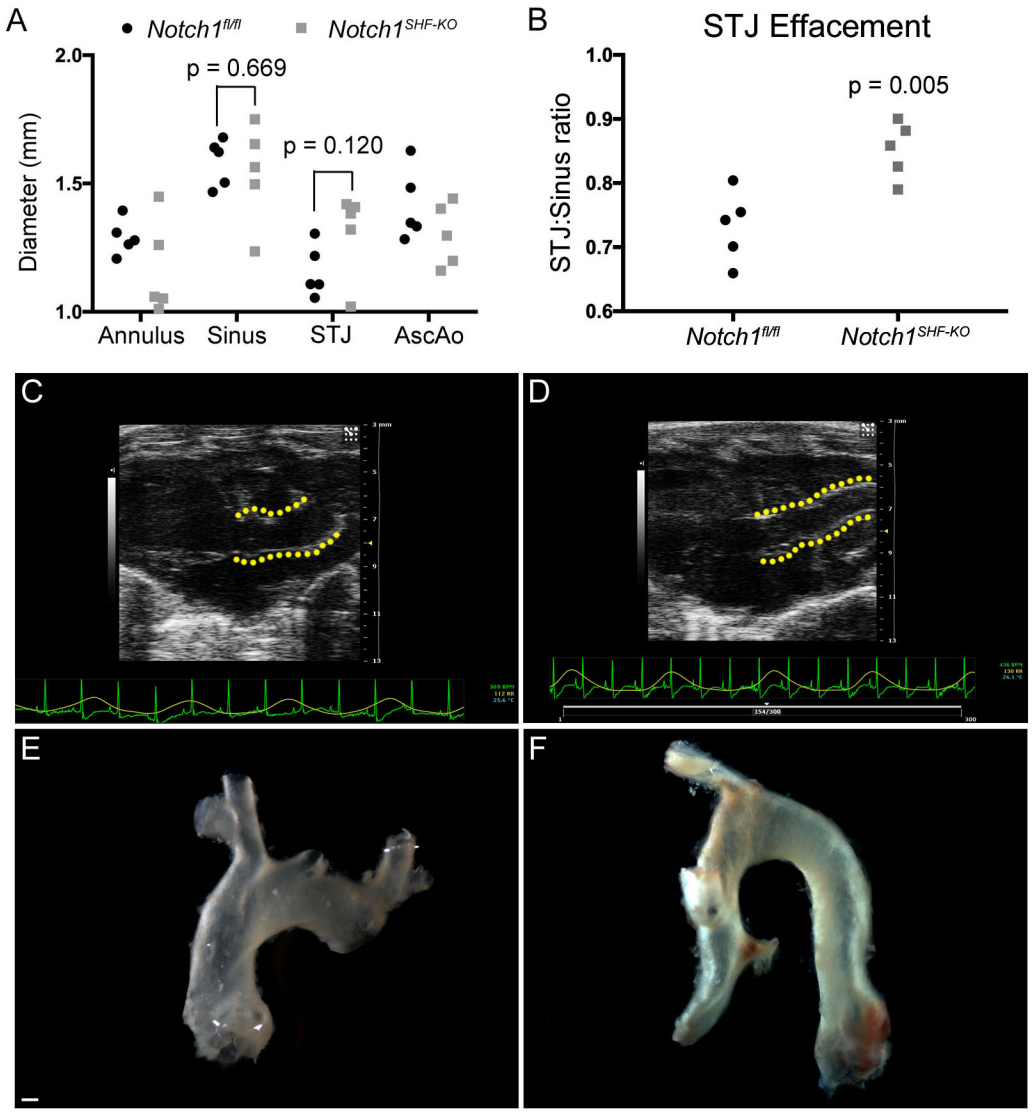

Supplemental Figure 5

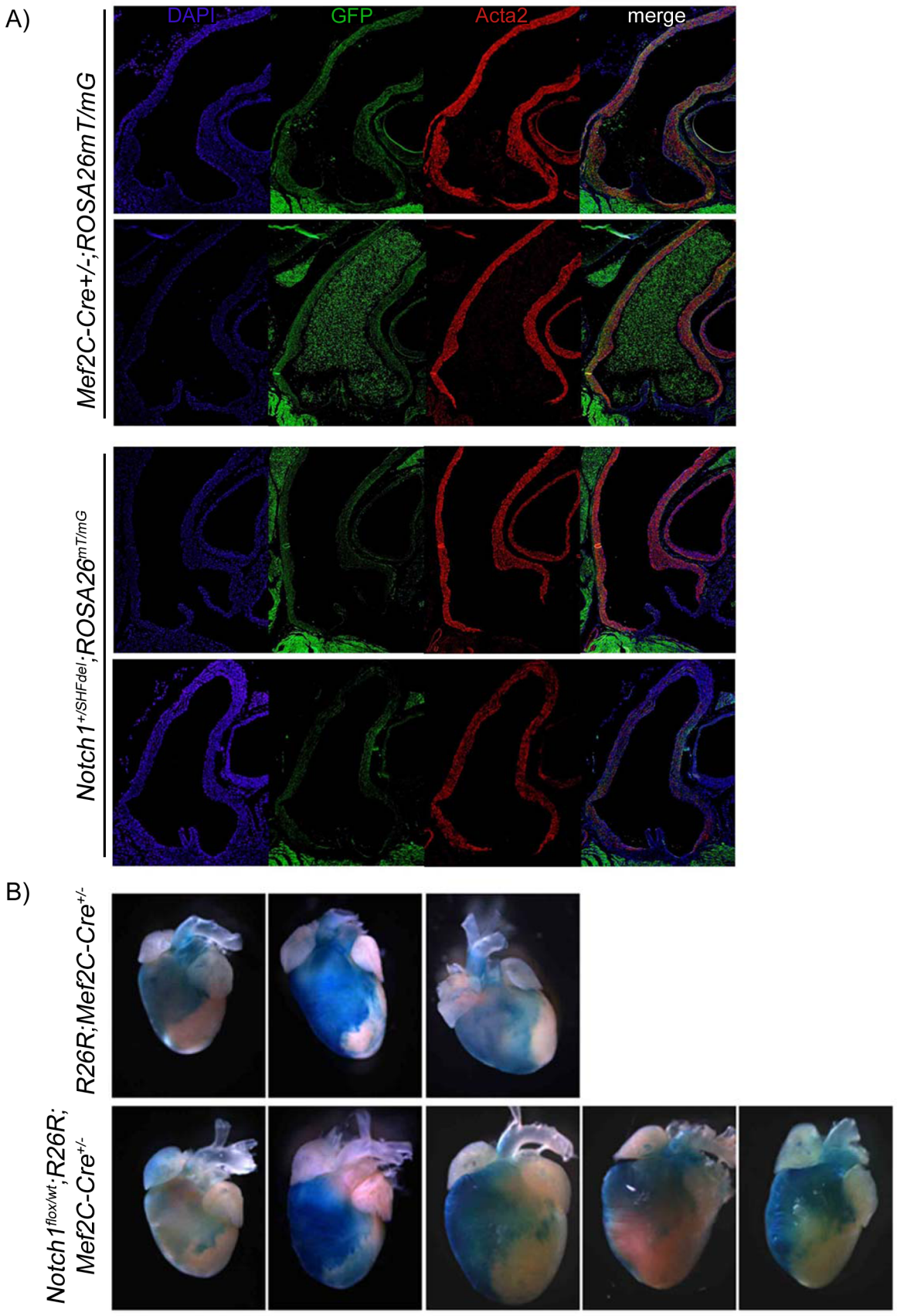

Supplemental Figure 6

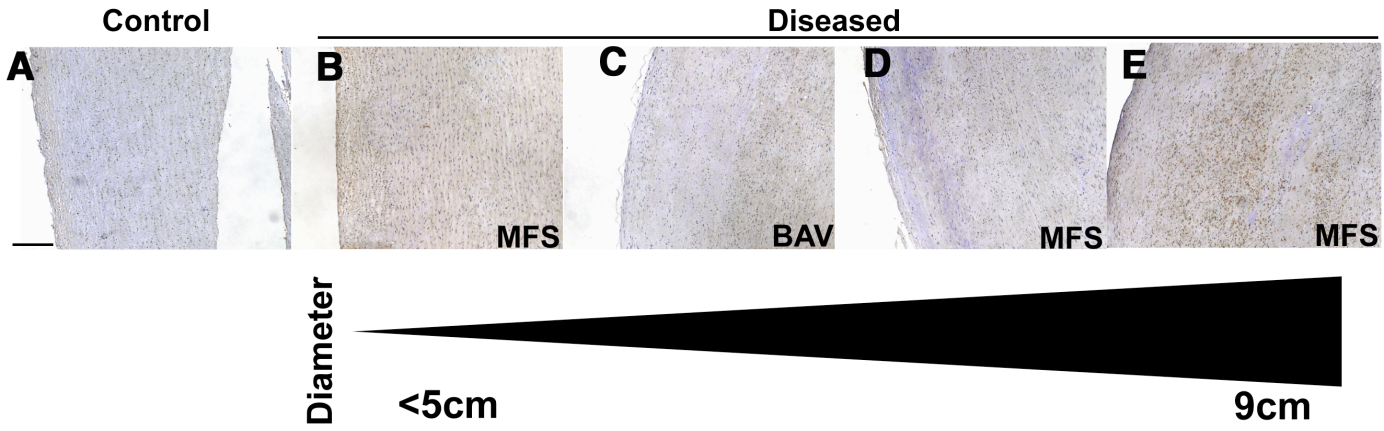

Supplemental Figure 7

Supplemental Table 1: Summary of cell-specific *Notch1*$^{+/-}$ in MFS mice

Lineage (promoter)	Dilated aorta	Aortic Rupture	# of *Notch1*$^{+/fl}$;*Cre*$^{+/-}$;*Fbn1*$^{C1039G/+}$ mice
Endothelial (Tie2)	No	No	10
Smooth muscle (Myh11)	No	No	17
Smooth muscle (Myocardin)	Yes	No	4
Second heart field (Mef2C)	Yes	Yes	8
Neural Crest (Wnt1)	No	No	10

Supplemental Table 2: Lethality of *Notch1*$^{SHF\text{-}KO}$ mice

Genotype of litters from breeding: *Notch1*$^{+/fl}$;*Mef2C-Cre*$^{+/-}$ x *Notch1*$^{fl/fl}$				
	Notch1$^{+/fl}$	*Notch1*$^{fl/fl}$	*Notch1*$^{+/fl}$; *Mef2C-Cre*$^{+/-}$	*Notch1*$^{SHF\text{-}KO}$
P21	102 (35%)	94 (32%)	92 (31%)	6 (2%)
E18.5	13 (19%)	23 (34%)	17 (25%)	14 (21%)
E15.5	4 (11%)	12 (34%)	8 (23%)	11 (31%)

Supplemental Table 3: Incidence of cardiac outflow tract defects in *Notch1*$^{SHF\text{-}KO}$ embryos

	Notch1$^{fl/fl}$	*Notch1*$^{SHF\text{-}KO}$
Double outlet right ventricle with ventricular septal defect	0/4	2/4
Persistent truncus arteriosus	0/4	1/4
Normal cardiac outflow tract	4/4	1/4